Specialty area: Quantitative Imaging and Modeling

Dr. rer. nat. Ellen Ackerstaff *ackerste@mskcc.org*

Highlights

1. Dynamic contrast enhancement modeling is influenced by data acquisition and choice of contrast agent.
2. Semiquantitative measures of contrast enhancement, while easily obtained and affected by the underlying tissue physiology, do not have necessarily straightforward physiological meaning, as they reflect a combination of tissue properties, such as tissue blood volume, vascular permeability, and volume of leakage space, and depend on experimental variables.
3. Quantitative DCE models are typically two-compartment models that estimate tissue perfusion and capillary permeability, permitting the straightforward physiological interpretation of vascular events in a tissue. However, special care has to be taken in the selection of the most appropriate model, in order to fulfill the underlying assumptions affected by contrast agent choice, tissue features, and data acquisition.

Modeling Dynamic Contrast Enhancement (DCE)

- **Target Audience:**
  Preclinical and clinical researchers, as well as clinicians, who analyze and interpret dynamic contrast-enhanced (DCE) magnetic resonance imaging (MRI) data that have been acquired to evaluate vascularity
  - during tumor progression and in response to treatments (chemo- and/or radiotherapy),
  - in the course of developing novel acquisition techniques, or
  - in other diseases characterized by vascular abnormalities

  While this presentation focuses on the analysis and interpretation of DCE-MRI data, the basic principles can be applied to other imaging modalities, such as DCE computed tomography (CT), ultrasound (US), single-photon emission tomography (SPECT), and positron emission tomography (PET) studies ([1] and references therein, [2]).

- **Outcome/Objectives:** The goal is to help the researcher to choose the most appropriate model to address a research/clinical question, based on the interpretation of calculated model parameters, and correspondingly choose the most suitable acquisition method, or *vice versa* choose an appropriate model for the analysis of existing DCE data.

- **Purpose:** The goal of modeling dynamic contrast enhancement is to elicit – based on contrast agent uptake behavior – vascular parameters and/or changes that are specific to the disease and/or its treatment response, and also are of physiological/biological relevance. There have been a number of reviews, addressing data acquisition and analysis of contrast enhancement in magnetic resonance imaging (e.g. [1, 3-6]). After a brief introduction of a variety of semiquantitative parameters that have been used to characterize contrast enhancement behavior, this lecture will focus on tracer kinetic models, applied either to voxel-by-voxel or regional average signal-to-time curves.

- **DCE Data Acquisition:** Typically, dynamic contrast enhancement is measured after the bolus injection of a contrast agent (CA) into a vein, with the degree of enhancement related to the CA concentration. The CA of choice is often a small inert molecule (low molecular weight contrast agent (LMWCA)) that remains extracellular. However, studies with targeted contrast agents which are taken up and metabolized by cells are of interest for treatment studies[7]. Macromolecular weight CAs (blood pool agents, MMCA) stay not only extracellular but also stay inside of healthy blood vessels, thus, are uniquely suitable

to visualize the vasculature, and are often used to assess vascular permeability in diseases characterized by leaky vasculature, such as cancer [5, 8, 9]. The qualities and features of various LMWCAs and MMWCAs have been reviewed in detail elsewhere[5, 8, 9].

The first pass of the CA uptake is characterized by the venous input function (VIF) / aterial input function (AIF)[1, 3, 10, 11]. After that the CA distributes throughout the vasculature, extravasates at sites of leaky blood vessels – such as in tumors – into the interstitium, and is ultimately cleared from the body. Rate and path (e.g. liver, kidney) of tissue and vascular clearance are dependent on the specific CA (e.g. size and type of CA)[8, 12].

The acquisition of dynamic contrast enhancement is dependent on the vascular features imaged and the contrast agent used. For example, measuring the VIF or AIF requires acquisition of DCE with high temporal resolution with a vein or artery in the field-of-view (FOV). When this is not practically feasible, which is often the case in preclinical models, population averages have been measured to be used in DCE data modeling[1, 10]. Following DCE in the region of interest (ROI) with sufficient temporal and spatial resolution to assess contrast enhancement in tissue regions of interest has become standard in the clinic and in preclinical studies[3, 6]. However, temporal and spatial resolutions are inversely related to each other, and both will depend on the imaging method's sensitivity to reproducibly assess signal enhancement. DCE acquisition methods that make use of compressed sensing[13, 14] may significantly improve temporal and spatial resolution[15-17]. In MRI, there are three acquisition methods to measure the contrast enhancement dynamically: (i) DCE-MRI, which exploits the shortening of the T_1 relaxation time of water protons near the CA, typically a Gd-based CA, (ii) dynamic susceptibility contrast (DSC)-MRI, which takes advantage of the effect of the CA (e.g. Gd-based CA or superparamagnetic iron oxide (SPIO) particles) on the T_2 and T_2^* relaxation time of nearby water protons[18], and (ii) Arterial spin labeling (ASL) MRI, where magnetically labeled water protons serve as endogenous "CA"[19]. For the purposes of this lecture, the focus will be on DCE-MRI only, while where DSC-MRI and ASL are concerned, the interested reader is referred to the literature (e.g. [18-25]).

- **Quantification and modeling of DCE-MRI data:** The signal-to-time curves of DCE data follow qualitatively several distinct curve shapes: (i) fast wash in followed by fast wash out, (ii) fast wash in followed by either slow by slow accumulation, or little or no wash out during the acquisition time, (iii) slow accumulation of the CA, and (iv) no CA uptake [1, 3, 26].

  Easy to calculate and convenient semiquantitative measures of signal enhancement behaviors include for example the wash-in slope, wash-out slope, time-to-peak (TTP), and initial area under the enhancement curve at a specific time (e.g. 90 s) after injection of the

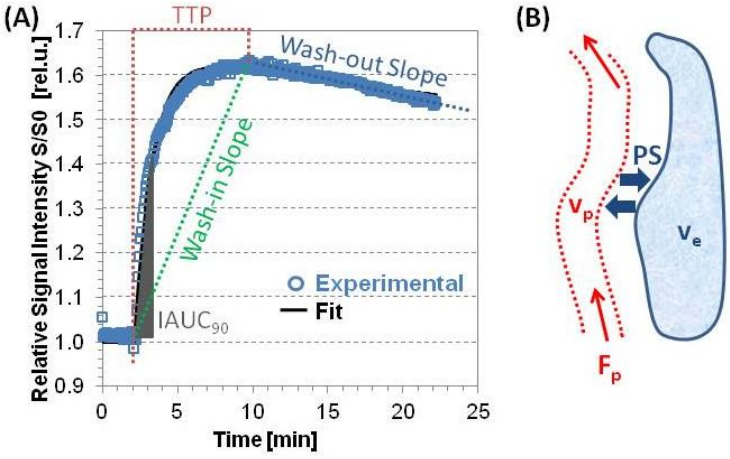

Figure 1: (A) Representative normalized signal-to- time curve of DCE-MRI data, and commonly calculated semiquantitative hemodynamic parameters. The CA was injected as a bolus at two minutes into the DCE-MRI data acquisition. (B) DCE data models: Schematic depicting the two tissue compartments accessible to CA and their CA exchange/flow parameters.

CA ($IAUC_{90}$), (**Figure 1A**)[3, 6]. Also, fractions of voxels with a degree of enhancement above a given threshold, using for example muscle to obtain the background reference threshold, are calculated to characterize the ROI[27]. Though, these semiquantitative measures are affected by the underlying physiology, they do not necessarily have straightforward physiological meaning, as they reflect a combination of tissue properties, such as tissue blood volume, vascular permeability, and volume of leakage space, and depend on experimental variables[3, 26]. The advantage of this approach to analyzing DCE data is that it does not require the knowledge of an AIF (or VIF)[3].

Pharmacokinetic models: The underlying principle of tracer kinetic modeling is the same for any dynamic imaging modality and is based on standard tracer-kinetic theory of linear and stationary systems[4, 28]. However, the kinetic of the CA can vary considerably and thus details in the model have to be adjusted. As reviewed in detail recently by Sourbron and Buckley, for DCE-MRI based on T_1-weighted imaging with a LMWCA (e.g. Gd-DTPA) a number of tracer-kinetic models have been developed[1, 29]. The assumptions are that the signal change measured after administration of the CA is directly related to the CA concentration in the voxel and independent of the injected concentration. The conversion of signal enhancement to CA concentration is hampered in DCE-MRI by its non-linear nature. Thus, often the relative signal enhancement over time $S(t)/S_0$, with S_0 depicting the precontrast signal, is used to approximate the CA concentration[1]. Another approach is to convert the signal S(t) into T_1 relaxation rates $R_1(t)$, with the difficulty of having to account for errors induced by (i) assumptions for water exchange across physical barriers, such as vessel walls, (ii) measurement of an AIF, due to CA bolus dispersion, inflow effects of excited proton spins in the imaging voxel, or non-linearity of CA concentration to signal enhancement at high CA concentrations, and (iii) other factors, such as B1 inhomogeneities[1].

Typically, inert, extracelluar CAs are used for DCE studies. Thus, a two-compartment model is used to describe the microcirculation in tissue (**Figure 1B**). The two compartments are the intravascular, extracellular space (blood plasma (BP), v_p) and extravascular, extracellular space (interstitium, v_e). The tissue vascularity can be described with the 4 independent parameters v_e, v_p, F_p, PS (**Table 1**), where Fp is the plasma flow and PS is the CA exchange rate between v_p and v_e, respectively. From these other hemodynamic parameters, such as K^{trans} or MTT, can be derived (**Table 1**). Starting with the development of the first generation kinetic models to analyze DCE-MRI data by Hoffman-Brix, Tofts, and Kety[30, 31] in the 1990s, various 2-compartment models of different complexity have been developed further by making differing assumption about CA exchange between and CA distribution within v_e and v_p[1, 29]:

Capillary or plasma models: The *compartment model* assumes that the CA concentration within a volume of interest is homogeneous and CA outflow is directly proportional to the CA concentration. The *plug-flow model* assumes that all CA molecules travel with the same velocity.

Two-region exchange models: The *2-compartment exchange model* assumes that the CA is homogeneously distributed within v_e and v_p, and that v_e exchanges CA only with v_p with the influx of CA into v_p equal to the outflux. The *tissue homogeneity model (TH)* uses the plug-flow model to describe the plasma volume, while all other assumptions are identical to the 2-compartment exchange model. The *adiabatic approximation to the tissue homogeneity model (AATH)* assumes that the capillary walls are impermeable to CA and that v_e only exchanges CA with v_p on the venous end of the capillary. With these simplifying assumptions to the TH model result in differential equations that can be solved in the time-domain, contrary to the TH model. The *distributed-parameter model* assumes

the plug-flow system for the capillary bed, and that the CA exchange with v_e, which is assumed to be comprised of a series of infinitesimal compartments, occurs only across the capillary wall, while there is no CA exchange between the compartments within v_e.

Often it is not possible to reliably model the 4 independent parameters, defining the models described above, based on the acquired DCE data. For example, in the brain an intact blood brain barrier inhibits the exchange of CA with v_e and, thus, no information about v_e is provided by the data. In such cases, additional assumptions are made reducing the number of independent variables, resulting in a variety of commonly applied models to fit DCE data:

Two-compartment uptake models are defined by the parameters F_p, v_p, and PS, as they assume that within the DCE data acquisition time the CA outflow from v_e is negligible, based on a small PS and/or a large v_e.

The ***extended Tofts model*** assumes that F_p is infinite, resulting in a concentration of CA molecules that did not extravasate proportional to the arterial CA concentration, and is defined by the parameters v_p, PS, and v_e.

The ***one-compartment model*** is defined by a volume v with a homogeneous CA distribution and the in- and outflow F. This model is suitable in situations where there is no CA exchange between the two compartments, or where the CA exchange is so fast that the compartments cannot be distinguished from each other and appear as one, or where the plasma volume v_p is negligible.

Table 1: Definitions of common hemodynamic parameters in DCE-MRI data modeling

Parameter	Definition	Unit
v_e	Interstitial volume	ml
v_p	Intravascular plasma volume	ml
F_p	Plasma flow, i.e. volume of plasma that enters a unit of tissue volume per unit time	min^{-1}
PS	Permeability surface area product, i.e. rate of exchange between v_e and v_p (number of CA molecules (mmol) that extravasate per unit of time (min) and plasma concentration (M) and tissue volume (ml)	min^{-1}
E	Extraction fraction, i.e. % of extravasating CA molecules	%
K^{trans}	Volume transfer coefficient (product of E and F_p)	min^{-1}
MTT	Mean transit time	min

The models described above assume that the water exchange across physiological barriers, such as the vessel wall or cell membranes, is fast. However, this may not be always correct. Thus, the shutter-speed model has been developed to account for experimental conditions where the transendothelial or transcytolemmal water exchange varies from the fast-exchange limit to the slow-exchange limit[32, 33].

For special cases, where an AIF or VIF is not readily available, reference region models have been developed to analyze DCE data[34-36]. These models use a well-characterized reference region, such as healthy muscle, in lieu of an AIF to calibrate signal intensity changes.

Using the models described above to analyze DCE data on a voxel-by-voxel basis permits to evaluate tissue heterogeneity of hemodynamic parameters at the cost of the contrast-to-noise ratio (CNR). While modeling average DCE curves of selected ROIs improves fitting, due to improved CNR, it potentially hides sub-regional vascular events by cancelling out enhancement loss due to CA washout in some voxels with enhancement increase due to CA accumulation in other voxels in the ROI. Identifying regions characterized by their

shape of contrast enhancement curves can improve the identification of sub-regional vascular events, while still benefitting from increased CNR of average contrast enhancement curves, and thus, promote relating modeled parameters to tissue/disease physiology and/or treatment response[3, 37].

- **Discussion and Conclusion:** The choice of model used to analyze DCE-MRI data depends on the tissue physiology (e.g. blood brain barrier, inhibiting extravasation of CA *versus* leaky tumor vasculature, leading to fast extravasation of CA into the interstitium), CA used (low molecular weight *versus* macromolecular weight), and DCE data acquisition (finding the optimal balance between time resolution, spatial resolution, total acquisition time, and CNR), as different assumption have to be fulfilled to calculate biologically meaningful hemodynamic parameters. Keeping the above in mind, DCE data modeling is a powerful tool to evaluate vascular events associated with disease physiology and treatment response.

References:

1. Ingrisch, M. and S. Sourbron, *Tracer-kinetic modeling of dynamic contrast-enhanced MRI and CT: a primer.* J Pharmacokinet Pharmacodyn, 2013. **40**(3): p. 281-300.
2. Logan, J., *Graphical analysis of PET data applied to reversible and irreversible tracers.* Nucl Med Biol, 2000. **27**(7): p. 661-70.
3. Barnes, S.L., et al., *Practical dynamic contrast enhanced MRI in small animal models of cancer: data acquisition, data analysis, and interpretation.* Pharmaceutics, 2012. **4**(3): p. 442-78.
4. Sourbron, S.P. and D.L. Buckley, *Tracer kinetic modelling in MRI: estimating perfusion and capillary permeability.* Phys Med Biol, 2012. **57**(2): p. R1-33.
5. Ocak, I., et al., *The biologic basis of in vivo angiogenesis imaging.* Front Biosci, 2007. **12**: p. 3601-16.
6. Leach, M.O., et al., *The assessment of antiangiogenic and antivascular therapies in early-stage clinical trials using magnetic resonance imaging: issues and recommendations.* Br J Cancer, 2005. **92**(9): p. 1599-610.
7. Neeman, M., et al., *Molecular imaging of angiogenesis.* J Magn Reson Imaging, 2007. **25**(1): p. 1-12.
8. Geraldes, C.F. and S. Laurent, *Classification and basic properties of contrast agents for magnetic resonance imaging.* Contrast Media Mol Imaging, 2009. **4**(1): p. 1-23.
9. Barrett, T., et al., *Macromolecular MRI contrast agents for imaging tumor angiogenesis.* Eur J Radiol, 2006. **60**(3): p. 353-66.
10. Loveless, M.E., et al., *A quantitative comparison of the influence of individual versus population-derived vascular input functions on dynamic contrast enhanced-MRI in small animals.* Magn Reson Med, 2012. **67**(1): p. 226-36.
11. Pathak, A.P., D. Artemov, and Z.M. Bhujwalla, *Novel system for determining contrast agent concentration in mouse blood in vivo.* Magn Reson Med, 2004. **51**(3): p. 612-5.
12. Barrett, T., et al., *MRI of tumor angiogenesis.* J Magn Reson Imaging, 2007. **26**(2): p. 235-49.
13. Candes, E.J. and Y. Plan, *Matrix Completion With Noise.* Proceedings of the Ieee, 2010. **98**(6): p. 925-936.
14. Donoho, D.L., *Compressed sensing.* Ieee Transactions on Information Theory, 2006. **52**(4): p. 1289-1306.
15. Adluru, G., et al., *Reconstruction of 3D dynamic contrast-enhanced magnetic resonance imaging using nonlocal means.* J Magn Reson Imaging, 2010. **32**(5): p. 1217-27.
16. Smith, D.S., et al., *Quantitative effects of using compressed sensing in dynamic contrast enhanced MRI.* Phys Med Biol, 2011. **56**(15): p. 4933-46.

17. Han, S., et al., *Temporal/spatial resolution improvement of in vivo DCE-MRI with compressed sensing-optimized FLASH.* Magn Reson Imaging, 2012.
18. Calamante, F., *Perfusion MRI using dynamic-susceptibility contrast MRI: quantification issues in patient studies.* Top Magn Reson Imaging, 2010. **21**(2): p. 75-85.
19. Detre, J.A., et al., *Tissue specific perfusion imaging using arterial spin labeling.* NMR Biomed, 1994. **7**(1-2): p. 75-82.
20. Knutsson, L., F. Stahlberg, and R. Wirestam, *Absolute quantification of perfusion using dynamic susceptibility contrast MRI: pitfalls and possibilities.* MAGMA, 2010. **23**(1): p. 1-21.
21. Paulson, E.S. and K.M. Schmainda, *Comparison of dynamic susceptibility-weighted contrast-enhanced MR methods: recommendations for measuring relative cerebral blood volume in brain tumors.* Radiology, 2008. **249**(2): p. 601-13.
22. Brix, G., R. Lucht, and J. Griebel, *Tracer kinetic analysis of signal time series from dynamic contrast-enhanced MR imaging.* Biomed Tech (Berl), 2006. **51**(5-6): p. 325-30.
23. Golay, X. and E.T. Petersen, *Arterial spin labeling: benefits and pitfalls of high magnetic field.* Neuroimaging Clin N Am, 2006. **16**(2): p. 259-68, x.
24. Golay, X., J. Hendrikse, and T.C. Lim, *Perfusion imaging using arterial spin labeling.* Top Magn Reson Imaging, 2004. **15**(1): p. 10-27.
25. Norris, D.G., *High field human imaging.* J Magn Reson Imaging, 2003. **18**(5): p. 519-29.
26. Walker-Samuel, S., M.O. Leach, and D.J. Collins, *Evaluation of response to treatment using DCE-MRI: the relationship between initial area under the gadolinium curve (IAUGC) and quantitative pharmacokinetic analysis.* Phys Med Biol, 2006. **51**(14): p. 3593-602.
27. Bradley, D.P., et al., *Correlation of MRI biomarkers with tumor necrosis in Hras5 tumor xenograft in athymic rats.* Neoplasia, 2007. **9**(5): p. 382-91.
28. Koh, T.S., et al., *Fundamentals of tracer kinetics for dynamic contrast-enhanced MRI.* J Magn Reson Imaging, 2011. **34**(6): p. 1262-76.
29. Sourbron, S.P. and D.L. Buckley, *Classic models for dynamic contrast-enhanced MRI.* NMR Biomed, 2013. **26**(8): p. 1004-27.
30. Tofts, P.S., et al., *Estimating kinetic parameters from dynamic contrast-enhanced T(1)-weighted MRI of a diffusable tracer: standardized quantities and symbols.* J Magn Reson Imaging, 1999. **10**(3): p. 223-32.
31. Hoffmann, U., et al., *Pharmacokinetic mapping of the breast: a new method for dynamic MR mammography.* Magn Reson Med, 1995. **33**(4): p. 506-14.
32. Buckley, D.L., L.E. Kershaw, and G.J. Stanisz, *Cellular-interstitial water exchange and its effect on the determination of contrast agent concentration in vivo: dynamic contrast-enhanced MRI of human internal obturator muscle.* Magn Reson Med, 2008. **60**(5): p. 1011-9.
33. Li, X., W.D. Rooney, and C.S. Springer, Jr., *A unified magnetic resonance imaging pharmacokinetic theory: intravascular and extracellular contrast reagents.* Magn Reson Med, 2005. **54**(6): p. 1351-9.
34. Yankeelov, T.E., et al., *Incorporating the effects of transcytolemmal water exchange in a reference region model for DCE-MRI analysis: theory, simulations, and experimental results.* Magn Reson Med, 2008. **59**(2): p. 326-35.
35. Kovar, D.A., M. Lewis, and G.S. Karczmar, *A new method for imaging perfusion and contrast extraction fraction: input functions derived from reference tissues.* J Magn Reson Imaging, 1998. **8**(5): p. 1126-34.
36. Lammertsma, A.A., et al., *Comparison of methods for analysis of clinical [11C]raclopride studies.* J Cereb Blood Flow Metab, 1996. **16**(1): p. 42-52.
37. Stoyanova, R., et al., *Mapping Tumor Hypoxia In Vivo Using Pattern Recognition of Dynamic Contrast-enhanced MRI Data.* Transl Oncol, 2012. **5**(6): p. 437-47.